Letter

Coiled-Coils in Phage Display Screening: Insight into Exceptional Selectivity Provided by Molecular Dynamics

Jérémie Mortier,[*,†,§] Elisabeth K. Nyakatura,[†,§] Oliver Reimann,[†] Susanne Huhmann,[†] Jan O. Daldrop,[‡] Carsten Baldauf,[||] Gerhard Wolber,[†] Markus S. Miettinen,[‡] and Beate Koksch[*,†]

[†]Department of Biology, Chemistry and Pharmacy, Freie Universität Berlin, Takustraße 3, 14195 Berlin, Germany
[‡]Department of Physics, Freie Universität Berlin, Arnimallee 14, 14195 Berlin, Germany
[||]Fritz Haber Institute der MPG, Faradayweg 4-6, 14195 Berlin, Germany

S *Supporting Information*
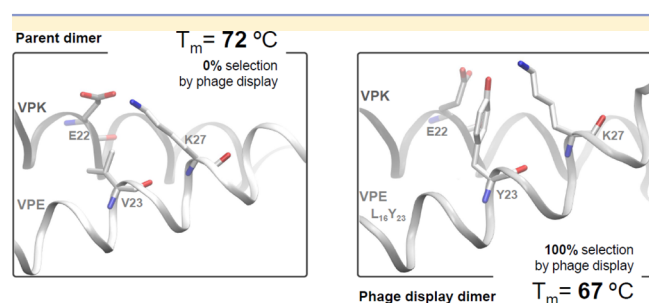
ABSTRACT: Involved in numerous key biological functions, protein helix—helix interactions follow a well-defined intermolecular recognition pattern. The characteristic structure of the α-helical coiled-coil allows for the specific randomization of clearly defined interaction partners within heteromeric systems. In this work, a rationally designed heterodimeric coiled-coil was used to investigate potential factors influencing the sequence selectivity in interhelical interactions.

Mutual recognition between two molecular patterns and the strength of this interaction are key factors for most biological functions. One recognition motif for hetero- and homoassembly that is utilized by nature is the specific interface of helix—helix interactions found in coiled-coil assemblies. The primary structure of coiled-coils is based on a characteristic heptad repeat of amino acids, whose seven positions are denoted as $a-b-c-d-e-f-g$.[1] Positions a and d are typically occupied by hydrophobic residues in these assemblies, enabling formation of the hydrophobic core and oligomerization. Residues at positions e and g are commonly charged and engage in interhelical electrostatic interactions.

The de novo designed VPK/VPE model system forms parallel coiled-coil heterodimers (Figure 1).[2−4] Heteromerization is facilitated by the introduction of $e−g'$ and $g−e'$ pairs that engage in favorable electrostatic interactions in the heteromer but would repel one another in either homomer. Valine is positioned in all a-positions to induce dimerization, since β-branched amino acids in a-positions are known to stabilize parallel coiled-coil dimers.[5] An additional stabilization element for the heteromeric parallel orientation is provided by reversing, at one site (g_{22} and e_{27} of VPK and g_{22}' and e_{27}' in VPE), the otherwise absolute lysine (g) glutamic acid (e') pattern. This

well-defined and thoroughly characterized coiled-coil provides a suitable starting point for systematically investigating helical protein—protein interactions.

In an aqueous environment, the α-helices of the coiled-coil associate in such a way as to bury hydrophobic surface areas, forming the hydrophobic core. In the middle of the sequence of VPK (Figure 1), L_{19} is a residue that participates in this lipophilic interaction. In the sequence of its partner VPE, V_{16}, L_{19}, and V_{23} engage in packing interactions with L_{19} of VPK in a well-described "knobs-into-holes" manner.[5] The primary question initiating this work was whether a VPE variant including different residues in these specific positions could form a heterodimer with VPK and what the impact would be on the stability of the complex. To this end, all possible VPE variants at the positions a_{16}', d_{19}', and a_{23}' were screened by means of phage display using VPK as a target. The single enriched sequence isolated in this screen was further analyzed in vitro and by computational means. Unrestrained molecular dynamics (MD) as well as center-of-mass (COM) pulling simulations were conducted using an atomistic model with explicit solvent. Based on a case study applying phage display, this work aims at highlighting and discussing the subtle differences between stability and selectivity in the context of helix—helix interactions.

Following previously published approaches,[3,6,7] the phage-display-library design was based on randomization of the three central hydrophobic positions of VPE that interact directly with position d_{19} of VPK, namely a_{16}', d_{19}', and a_{23}' (Figure 1). VPE was displayed as a fusion with bacteriophage coat protein pIII and VPK was immobilized on streptavidin coated magnetic particles via an N-terminal biotin tag; this is expected to facilitate parallel helix alignment of the heteromeric assembly. A Gly-Ser-Gly stretch served as a spacer between the biotin moiety and the VPK sequence. The best binding partners from a phage-displayed library, which covered all 8000 (20^3) VPE variants by 4 orders of magnitude, were determined after five rounds of panning (see supporting Table S2).

VPK, harboring leucine at position d_{19}, was utilized as the target in the screen. Biopanning and subsequent sequencing of the amplified phagemid vectors revealed a single isolated consensus VPE sequence, containing leucines in positions a_{16}' and d_{19}' and tyrosine in position a_{23}' (Figure S1). Leucine is the
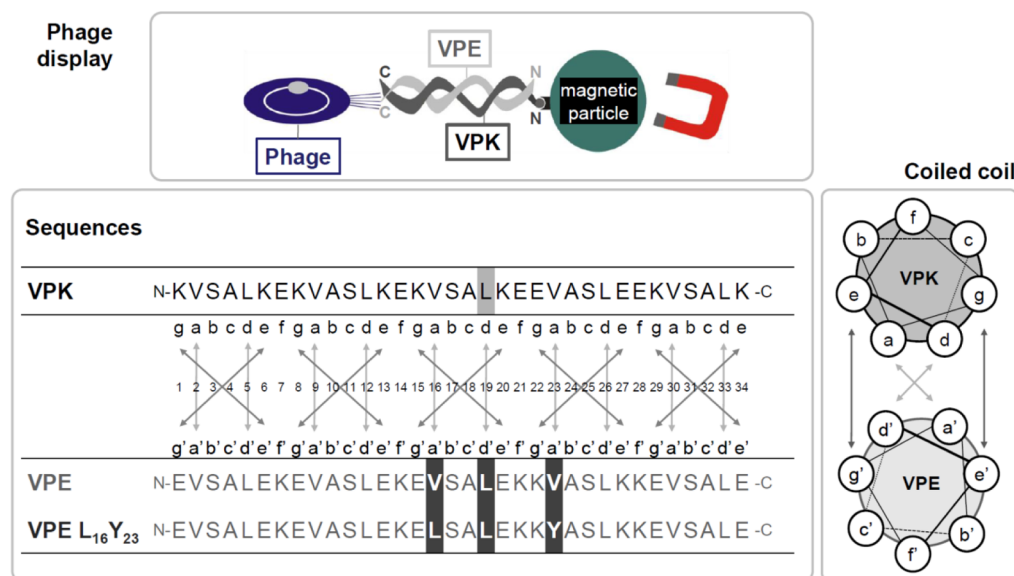
Figure 1. Graphical representation of the phage display experiment (upper left); aligned peptide sequences of VPK and VPE variants (lower left) with L19 of VPK highlighted in a light gray box and the three randomized positions in VPE highlighted by black boxes; helical wheel depiction of the coiled-coil dimer (right).
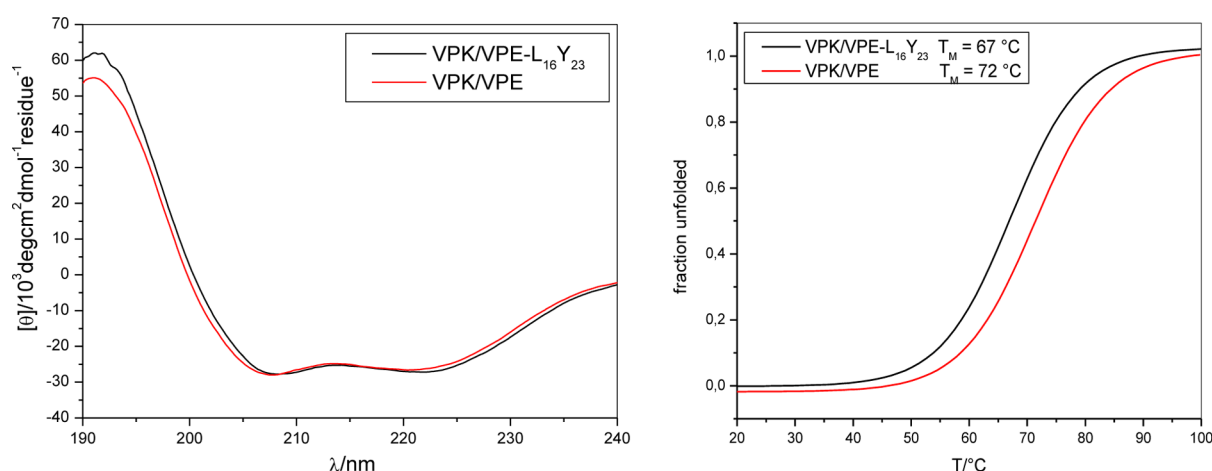

Figure 2. CD spectra of VPK/VPE$_{variant}$ heteromers depicted as the mean of three experiments (left) and thermal denaturation spectra (sigmoidal fit) of VPK/VPE$_{variant}$ heteromers (right): peptide conc. 20 μM; 100 mM phosphate buffer; pH 7.4. T_M standard deviations from three independent measurements were $\pm$0.1 °C.

predominant residue found in the d-positions of naturally occurring coiled-coil motifs,[8] and studies by Hodges et al.[9] identified leucine as the most favored amino acid, with regard to providing thermal stability, in the context of the d-positions of parallel α-helical coiled-coils. Thus, its selection at d_{19}' is not surprising. The selection of leucine in position a_{16}' might be attributed to the higher hydrophobicity compared to valine, which occupies all a-positions of VPK and parent VPE.[2] Surprisingly, the polar aromatic residue tyrosine was selected in position a_{23}' of VPE. In order to elucidate the intermolecular interactions that are responsible for this selection outcome, VPE-L$_{16}$Y$_{23}$ was chemically synthesized and further experimentally characterized in the context of the selected assembly VPK/VPE-L$_{16}$Y$_{23}$.

CD spectra obtained from a 1:1 mixture of VPK/VPE-L$_{16}$Y$_{23}$ clearly indicate two distinct minima, at 208 and 222 nm, and thus verify the formation of helical assemblies (Figure 2); moreover, they are nearly superimposable with the traces obtained from VPK/VPE, which is compatible with a similar

global conformation. Size exclusion chromatography (SEC) with detection based on static light scattering (SLS) shows that the dimeric oligomerization state of the VPK/VPE parent system is retained in the phage display variant (Figure S2). A shoulder of the size exclusion peak indicates a relatively small (<25%) proportion of trimeric species.[2,4] We note that the possibility that one VPK can select two VPE-L$_{16}$Y$_{23}$ peptides through the formation of trimers is unlikely to explain the selection of this particular sequence of VPE over the parent one, which is forming dimers only. This is due to the excess of VPK in the phage−target binding, which guarantees that both versions of VPE will always be able to find a binding partner. Seeking to determine the thermal stability of the selected assembly, the CD signal at 222 nm, which is distinctive for α-helices, was monitored with increasing temperature. The measured thermal stability of the VPK/VPE-L$_{16}$Y$_{23}$ bundle (T_M = 67 °C, Figure 2) is lower than that one of the parent VPK/VPE (T_M = 72 °C, Figure 2).[2,3] This result raises two central questions. First, in an environment with all possible
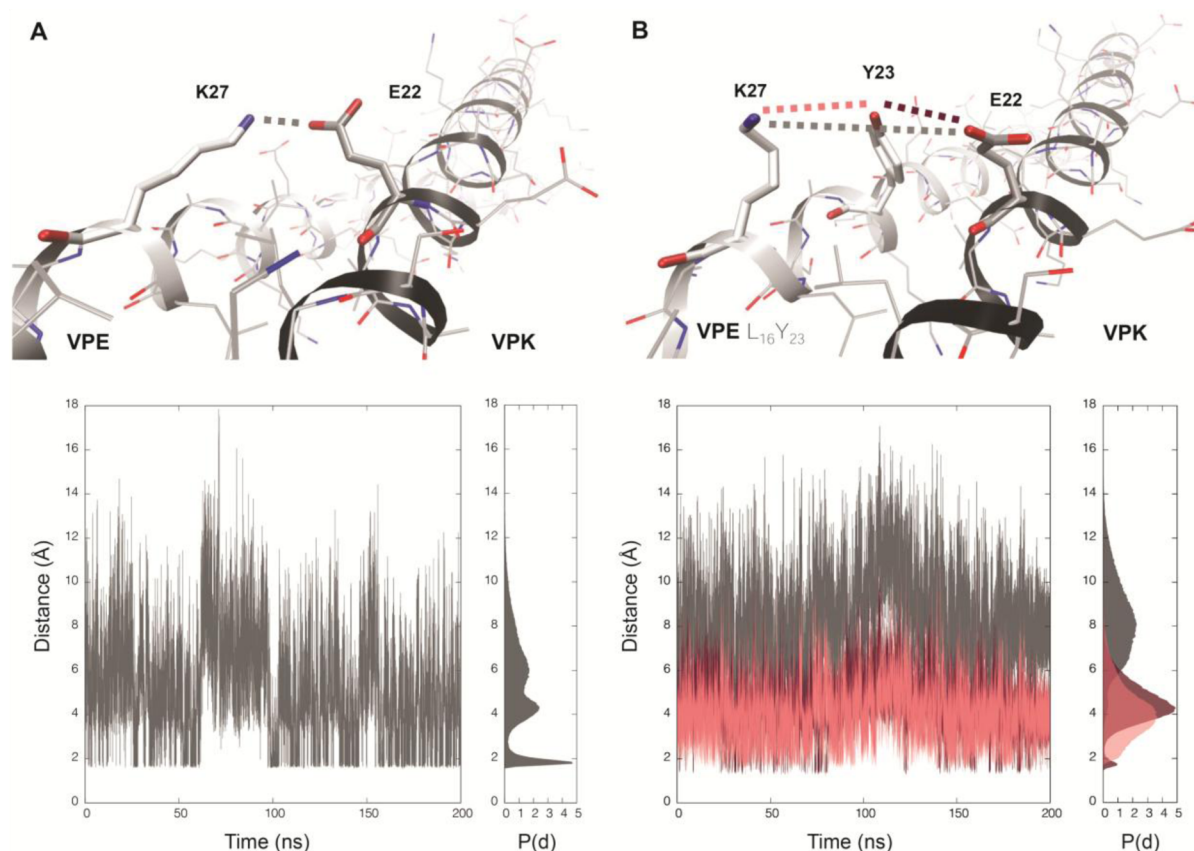
Figure 3. (top) 3D-Models of the parent dimer VPK/VPE (**A**) and the phage display variant VPK/VPE-$L_{16}Y_{23}$ (**B**). (bottom) Distances analysis for representative 200 ns windows and probability distributions $[P(d)]$ for the full simulation. Measurements involving K_{27} are performed between the closest hydrogen of the group NH_3^+ and measurements involving E_{22} are performed between the closest oxygen of the COO^- to the hydroxyl group of Y_{23}.

VPE-variants (see supporting Table S2), why is VPK exclusively selecting a sequence of VPE that is not creating the most stable (in terms of thermal denaturation) intermolecular interaction? Second, what is the role of selected tyrosine 23, an atypical residue for the hydrophobic core of the coiled-coil? To address these key points on stability and selectivity, the two systems have been thoroughly investigated using a computational approach.

3D-Models were built for the dimers VPK/VPE (parent) and VPK/VPE-$L_{16}Y_{23}$ (phage display-selected variant) in parallel strand orientation to investigate specifically tyrosine a_{23}' and the potential interactions stabilizing this residue within the coiled-coil. Both models were constructed by aligning our systems to the crystal structure of a natural coiled-coil, the Rho-kinase (PDB code 1R48),[10] without constraint on the side chains. After minimization with explicit solvent, each dimer was simulated three times for 200 ns, using Gromacs with the Amber 99sb force field.[11,12] Trajectory analysis of the VPK/VPE-$L_{16}Y_{23}$ system reveals that, being situated at an *a*-position where the $C_\alpha-C_\beta$ bond vector points out of the hydrophobic core, the large hydrophobic surface of the tyrosine aromatic ring provides for exclusion of water at the nonpolar helical interface. In general, the formation of hydrophobic interfaces between two nonpolar side-chains leads to a loss of side chain conformational entropy.[13,14] In regard to this, tyrosine might be particularly favorable since its side-chain rotamers are restricted. Moreover, as observed early in the unconstrained MD simulations of VPK/VPE-$L_{16}Y_{23}$ (already in the first 5 ns of

simulation time), the hydroxyl group of the tyrosine is mostly in a distance range from 2 to 6 Å to the primary amine of VPE-K_{27} and 3 Å to 6 Å to the carboxyl group of VPK-E_{22} (Figure 3B). Even though such distances allow for hydrogen bonding with these two partners, H-bonds are observed during only 3.2% of the simulation time (2.6% for $Y_{23}-E_{22}$ and 0.6% for $Y_{23}-K_{27}$) using 3 Å cutoff for the distance and 20° the angle. Even using a looser cutoff (3,5 Å and 30°),[15] the H-bond occurrence reaches not more than 4.7% (Table 1).

Nevertheless, during the simulation, the hydroxyl group of the tyrosine is always observed between VPK-E_{22} and VPE-K_{27} in the phage display dimer with the angle $K_{27}-Y_{23}-E_{22}$ observed most of the time around 160° (Figure S4). This result indicates that water molecules might connect these three groups by H-bond bridges. The analysis of the trajectories

Table 1. Proportion of Simulation Time with a Detected H-Bond and Water Bridge

		hydrogen-bond		water bridge	
cutoffs for H-bond detection[a]		strict	loose	strict	loose
parent dimer	$K_{27}-E_{22}$	6%	12%	46%	58%
	$Y_{23}-K_{27}$	1%	5%	37%	58%
phage display dimer	$Y_{23}-E_{22}$	3%	4%	47%	67%
	$K_{27}-Y_{23}-E_{22}$	0%	1%	18%	38%

[a]"Strict" refers to a cutoff of 3.0 Å for the H-bond distance and 20° for the H-bond angle, and "loose", to 3.5 Å and 30°.

shows that water molecules indeed form H-bond with both Y_{23} and E_{22} for 67% of the simulation time and 58% with Y_{23} and K_{27} (Table 1). Furthermore, simultaneous water bridges between Y_{23}–K_{27} and Y_{23}–E_{22} occur 38% of the simulation time. We note that another important type of interaction that may occur between residues Y_{23} and a lysine is the π-cation interaction, which however is not well described by classical force fields. A π-cation interaction could take place between Y_{23} and lysines in its neighborhood, such as K_{21}, K_{22}, and K_{27} in VPE-$L_{16}Y_{23}$. As K_{21} and K_{22} are located in positions f' and g', on the other side of the hydrophobic core (Figure 1), their interaction with Y_{23} could impede the formation of the coiled-coil. Contrarily, as discussed previously, in the coiled-coil the e' residue K_{27} is in the neighborhood of a' Y_{23} (Figure 3B). Thus, should π-cation interactions play an important role in the stabilization of the coiled coil, the very result of the phage display screening indicates that the most likely π-cation interaction involving Y_{23} is the one with K_{27}. To sum up, the MD simulations of the phage display dimer reveal that these three side chains (K_{27}, Y_{23}, and E_{22}) interact through an water mediated dynamic H-bond cluster. This could explain how the phage-selected system stabilizes this particular tyrosine side chain at this particular position of the coiled-coil.

A model of parent VPK/VPE was also constructed and simulated under conditions identical to those used for the phage-display variant. Similarly, the coiled-coil structure was found to be stable during the 200 ns of simulations (data not shown). In the absence of the large a_{23}' tyrosine in the VPE sequence, the model shows that the side chains VPK-E_{22} and VPE-K_{27} can make contact (Figure 3A). Due to the length of their side chains and their solvent exposed position, these residues also have numerous degrees of freedom. As observed between 60 and 90 ns of simulation time in the plot reported in Figure 3A, the measured distances between the charged groups can fluctuate from 2 to 17 Å; however, most of the time, the polar heads of VPK-E_{22} and VPE-K_{27} are observed within 2–4 Å from one another, interacting with electrostatic interactions above the short chained valine in position a_{23}' of the hydrophobic core. As with the phage-display dimer, very few hydrogen bonds were detected between VPK-E_{22} and VPE-K_{27} (6.0% of the simulation time using strict cut-offs), and thus most of the time they interact through a water molecule intermediate (46% of the simulation time using the same cutoffs, Table 1). The absence of global structural change triggered by the presence of Y_{23} in the selected VPE variant correlates with the small difference observed in thermostability between VPK/VPE and VPK/VPE-$L_{16}Y_{23}$. So, even though the side chain of tyrosine is chemically quite different from that of valine, the main interactions stabilizing the heterodimer are not disturbed when tyrosine is introduced into this particular position in VPE (see also contact maps in Figure S5).

In an attempt to explain the selection of the variant VPE-$L_{16}Y_{23}$, the dimerization process of the two monomers was investigated by MD. Configurations were generated at selected centers-of-mass (COM) distances between the two helices, by maintaining the COM distance with a harmonic spring. At each COM distance, an independent simulation was conducted.

The last conformations from the unrestrained MD simulations reported above were used to initiate this study. The first step in silico aimed at separating the two monomers up to 30 Å from one COM to another. This conformation was then used as the initial conformation in all subsequent simulations. That is, from a distance of 30 Å, the two helices

VPE and VPK were pulled together to reach the desired COM distances ranging between 4.5 and 30 Å. Each COM distance was simulated for 30.5 ns and was repeated five times (using identical coordinates and a different seed for the random numbers for the velocities). We note that, although the orientation of the two monomers was not constrained in the simulations, the parallel orientation appears to be conserved in silico at all distances (Figure S6). An identical state to the original stable dimer is reached when the COM distance is ranging from 7 to 8 Å between the two monomers. Indeed, the measured root-mean-square deviation (RMSD) to the initial minimized structure considering all peptide atoms is between 5 and 6 Å for the window with COM distance set at 7.5 Å. A particular emphasis was then put on COM distances from 10 to 20 Å, where the two dimers would have their first contacts, i.e. we hope to see with which partners the side chain of residue Y_{23} from VPE-$L_{16}Y_{23}$ interact during the dimerization process. Intermolecular H-bonds were observed between the tyrosine hydroxyl group and side chains E_{22} and K_{15} of VPK, as were intramolecular H-bonds with E_{20} and K_{27} (data not shown). Bearing a valine in this position, the parent VPE peptide is unable to facilitate dimerization by means of such interactions. The unique chemical functionality of the tyrosine side chain enables it to combine H-bonding, via its polar protic "head", with hydrophobic contacts, via its aromatic "body", which suggests an explanation on how this residue could assist in the complexation process from a kinetic perspective.

In conclusion, the heterodimeric coiled-coil system VPK/VPE was utilized to investigate potential factors influencing the selectivity of interhelical interactions. Three central positions in the VPE sequence were randomized, yielding a library that was subjected to a phage-display screen. One VPE variant, VPE-$L_{16}Y_{23}$, was isolated, displaying 100% enrichment. Since the VPK/VPE-$L_{16}Y_{23}$ dimer has a lower thermostability than the parent VPK/VPE complex, a computational investigation was conducted to comprehend the dimerization process of these two systems. On the one hand, this work identifies potential stabilizing intermolecular interactions involving the Y_{23} residue in the phage-display variant, explaining why this particular sequence could be selected. On the other hand, the analysis of the peptide–peptide interactions with varying COM distance highlights the same residues, thus providing a preliminary hypothesis for the selection of VPE-$L_{16}Y_{23}$ despite its lower thermal stability (than VPE) when complexed with VPK. This work has allowed rationalization of an atypical experimental result in the field of phage-display screening. The outcome of this study highlights the complexity of a discussion involving selectivity vs stability in the context of protein–protein interactions; the approach reported here proposes computational solutions to investigate factors influencing selectivity at the level of specific intermolecular interactions.

■ EXPERIMENTAL SECTION

Peptide Synthesis. Peptide synthesis was carried out in a 0.05 mM scale on a Syro-XP-1 peptide synthesizer (Multi-SynTech GmbH, Witten, Germany) using standard Fmoc/tBu chemistry as described previously.[2] The coupling mixture contained 0.23 M $NaClO_4$ to prevent on-resin aggregation. N-Terminal coupling of biotin (Acros) was performed as double coupling using DIC/HOBt as coupling reagents and a 4-fold excess relative to the resin loading. Nonbiotionylated peptides were cleaved from the resin by treatment with 4 mL TFA/TIS/H_2O (95:2.5:2.5). Biotinylated peptides were cleaved from the

resin with TFA−TIS−EDT−H$_2$O (94:2.5:2.5:1) to prevent oxidation of biotin. Purification was carried out by RP-HPLC (Phenomenex, Luna C$_8$,10 mm, 250 nm × 21.2 mm). Purity and identity of the products was determined by analytical HPLC (Phenomenex, Luna C$_8$, 5 μm, 250 nm × 4.6 mm) combined with high resolution mass spectra (Agilent 6210 ESI-TOF mass spectrometer, Agilent Technologies, Santa Clara, CA, USA).

Construction of the VPE Library. Library construction was performed by annealing two complementary VPE encoding oligonucleotides in which the library codons are randomized applying the NNK-strategy.[16,17] The library DNA was cloned into the pComb3H27 phagemid vector (GenBank database accession number: AF268280, Barbas laboratory, TSRI) by SfiI sites and transformed into *E. coli* K12 ER2738 (New England Biolabs no. E4104S) as described previously.[3] The library size was calculated to be 1.2×10^7. Production of the phage library was carried out as previously described.[3]

Phage Selection and Amplification. For phage selection, approximately 10 nmol biotinylated target peptide was immobilized on 30 μL streptavidin-coated magnetic particles (M-280, Dynal Biotech). Particles were washed twice with 500 μL 0.1% Tween20 in PBS. 500 μL 5% nonfat dried milk in PBS was added and the sample was incubated at RT for 45 min. After removing the milk−PBS suspension, 500 μL phage solution were added and phage−target binding was performed for 1.5 h at RT. Subsequently, the particles were washed four times with 500 μL Tween20 in PBS (PBS buffer contained 0.1% Tween 20 in round 1; 1% Tween 20 in rounds 2−5; in round 5 two washing steps with 1 M GndHCl in PBS were added) and once with 500 μL TBS. Bound phages were eluted from magnetic particles by adding 25 μL freshly prepared trypsin solution (10 mg/mL in TBS) and incubation at RT. After 30 min the reaction was quenched with 75 μL SB medium. For reinfection the received phage suspension (100 μL) was transferred to 5 mL *E. coli* culture. After 30 min at 37 °C/200 rpm, 10 μL of the cell culture were removed to determine the phage output titer, and 5 mL prewarmed SB medium containing 2.5 μL carbenicillin (100 mg/mL) were added. Cells were incubated for 1 h at 37 °C/200 rpm and then transferred to 90 mL prewarmed SB medium to which 46 μL carbenicillin (100 mg/mL) and 1 mL VCSM13 helper phage (Stratagene no. 200251) were added. After another 1.5 h at 37 °C/200 rpm 140 μL kanamycin (50 mg/mL) were added and phages were produced overnight. The culture was centrifuged for 30 min at 4 °C and 3000 g, and phages were precipitated by the addition of 20 vol % PEG−NaCl [20% (w/v) PEG 8000, 2.5 M NaCl] to the supernatant. After incubation for 30 min on ice phages were centrifuged for 30 min at 4 °C and 12 000g. Isolated phages were suspended in PBS buffer and used in the following round of panning after sterile filtration (0.22 mm).

SE/SLS. Static light scattering data were collected on a Dawn Heleos 8 light scattering instrument (Wyatt Technology) coupled with an analytical gel filtration (workstation: La Chrom, VWR, Hitachi, L-2130; column WTC-015S5; 5 μm, 150 Å, 7.8 mm × 300 mm, Wyatt Technology) at λ = 220 nm. All measurements were performed at room temperature with a flow rate of 0.3 mL/min. Data were analyzed using the ASTRA software version 5.3.4.20 (Wyatt Technology). Measurements were taken at pH 7.4 from a 1:1 mixture of VPK/VPE-L$_{16}$Y$_{23}$ and carried out in triplicate to confirm reproducibility and give standard deviations. Peptide concentrations were determined

using the absorbance of *o*-aminobenzoic acid (λ_{max} = 320 nm at pH 7.4) as previously described.[2]

CD Spectroscopy. CD spectra were recorded on a Jasco J-715 spectropolarimeter at 20 °C (Jasco PTC-348 WI Peltier thermostat). Peptide concentrations were determined using the absorbance of *o*-aminobenzoic acid (λ_{max} = 320 nm at pH 7.4). For melting curves, the CD signal at 222 nm was recorded applying a heating rate of 3 K/min from 20 to 95 °C. All spectra were baseline corrected and each sample was prepared three times. The determination of T_M was carried out as described previously.[2]

Molecular Dynamics. Models of the coiled-coils VPK/VPE and VPK/VPE-L$_{16}$Y$_{23}$ were built using the software MOE.[18] The sequences of the investigated peptides were aligned to the coiled-coil structure of the RhoA-binding domain in Rho-kinase (PDB code 1R48),[10] and the residues were replaced manually following the characteristic a−b−c−d−e−f−g pattern. Using Gromacs (version 4.5.3)[11,19] with Amber99sb force field,[12] each coiled-coil (parent and phage display variant) was placed in a 376 nm^3 dodecahedron box filled with 12 110 explicit simple point charge (SPC) water molecules, to which 100 mM NaCl was added, including neutralizing counterions. Following steepest descent minimization, each of the coiled-coils was equilibrated for 0.1 ns using position restraints applied to all peptide heavy atoms. Then each system was simulated for 200 ns (time step length = 2 fs), with periodic boundary conditions, using PME electrostatics ($r_{coulomb}$ = 10 Å)[20] and van der Waals interactions cutoff (r_{vdw} = 10 Å). Constraints were used on all bonds in the peptides (LINCS algorithm).[21] The Nosé−Hoover coupling method was used (temperature of 300 K)[22,23] together with the Parrinello−Rahman coupling method (pressure of 1 bar).[24] Each system was simulated in triplicate with different seed numbers. To identify water bridges, water molecules that simultaneously formed hydrogen bonds with the corresponding donor/acceptor groups of the residues of interest were searched using the MDAnalysis package.[25]

The peptide structures at the end of the 200 ns trajectories were extracted and used as starting conformation for the fixed-COM-distance simulations. Each dimer (parent and phage display variant) was placed in a dodecahedron box with a volume around 1000 nm^3 filled with 31 720 explicit simple point charge (SPC) water molecules. The two helices of each system were first pulled apart up to 30.0 Å between their centers-of mass (COM). The resulting conformation of this first simulation was then used as a starting system to bring the two monomers together. Then each system was simulated at selected COM distances between 4.5 and 30.0 Å. Electrostatics, van der Waals interactions, and covalent bonds were described in the same way as for the free-COM-distance (200 ns) simulations. Each sample was simulated for 30.5 ns, and each experiment was repeated 5 times with different gen seed numbers. Time step length was 2 fs. The velocity-rescale coupling method was used to maintain temperature at 300 K,[26] and the Berendsen weak coupling method was used to maintain the pressure at 1 bar.[27] A quadratic form for the energy with a force constant of 10 kJ/mol·Å^2 was used to fix the COM distances.

■ ASSOCIATED CONTENT

Ⓢ Supporting Information
(1) Identification of the peptides by ESI-TOF mass spectrometry. (2) Construction of the VPE library. (3) Phage enrichment. (4) Experimental characterization of the hetero-

mers. (5) Calculated energy of the system. (6) Angle $K_{27}-Y_{23}-E_{22}$. (7) Contact maps. (8) Dimer model orientation. This material is available free of charge via the Internet at http://pubs.acs.org.

■ AUTHOR INFORMATION

Corresponding Authors

*E-mail: beate.koksch@fu-berlin.de. Fax: +49 30 83855644. Tel.: +49-030-83855344 (B.K.).
*E-mail: jeremie.mortier@fu-berlin.de. Tel.: +49 30 83858090 (J.M.).

Author Contributions

§J.M. and E.K.N. contributed equally to this work. Conception and design of phage display: E.K.N. Phage display, peptide synthesis, and peptide characterization: E.K.N., O.R., and S.H. Conception and design of MD: M.S.M., J.M., and C.B. Analysis and interpretation of the data: M.S.M., J.O.D, E.K.N., J.M., and C.B. Writing the manuscript: J.M and E.K.N. Critical revision: B.K. and G.W.

Notes

The authors declare no competing financial interest.

■ ACKNOWLEDGMENTS

■ REFERENCES

(1) Mclachlan, A. D.; Stewart, M.; Smillie, L. B. Sequence Repeats in Alpha-Tropomyosin. *J. Mol. Biol.* **1975**, *98*, 281−291.

(2) Salwiczek, M.; Samsonov, S.; Vagt, T.; Nyakatura, E.; Fleige, E.; Numata, J.; Cölfen, H.; Pisabarro, M. T.; Koksch, B. Position-Dependent Effects Of Fluorinated Amino Acids On The Hydrophobic Core Formation of a Heterodimeric Coiled Coil. *Chem.−Eur. J.* **2009**, *15*, 7628−7636.

(3) Vagt, T.; Nyakatura, E.; Salwiczek, M.; Jäckel, C.; Koksch, B. Towards Identifying Preferred Interaction Partners Of Fluorinated Amino Acids Within The Hydrophobic Environment of a Dimeric Coiled Coil Peptide. *Org. Biomol. Chem.* **2010**, *8*, 1382−1386.

(4) Nyakatura, E. K.; Reimann, O.; Vagt, T.; Salwiczek, M.; Koksch, B. Accommodating Fluorinated Amino Acids in Helical Peptide Environments. *RSC Adv.* **2013**, *3*, 6319−6322.

(5) Woolfson, D. N.; David, A. D.; Parry, A. J. M. S. The Design Of Coiled-Coil Structures and Assemblies. In *Advances in Protein Chemistry*; Academic Press, 2005; Vol. *70*, pp 79−112.

(6) Nyakatura, E. K.; Rezaei Araghi, R.; Mortier, J.; Wieczorek, S.; Baldauf, C.; Wolber, G.; Koksch, B. An Unusual Interstrand H-Bond Stabilizes The Heteroassembly Of Helical αβγ-Chimeras with Natural Peptides. *ACS Chem. Biol.* **2014**, *9*, 613−616.

(7) Nyakatura, E. K.; Mortier, J.; Radtke, V. S.; Wieczorek, S.; Rezaei Araghi, R.; Baldauf, C.; Wolber, G.; Koksch, B. β- and γ-Amino Acids at α-Helical Interfaces: Toward the Formation of Highly Stable Foldameric Coiled Coils. *ACS Med. Chem. Lett.* **2014**, *5*, 1300−1303.

(8) Lupas, A.; Van Dyke, M.; Stock, J. Predicting Coiled Coils From Protein Sequences. *Science* **1991**, *252*, 1162.

(9) Tripet, B.; Wagschal, K.; Lavigne, P.; Mant, C. T.; Hodges, R. S. Effects Of Side-Chain Characteristics On Stability And Oligomerization State Of A De Novo-Designed Model Coiled-Coil: 20 Amino Acid Substitutions in Position "D"●. *J. Mol. Biol.* **2000**, *300*, 377−402.

(10) Shimizu, T.; Ihara, K.; Maesaki, R.; Amano, M.; Kaibuchi, K.; Hakoshima, T. Parallel Coiled-Coil Association of the Rhoa-Binding Domain in Rho-Kinase. *J. Biol. Chem.* **2003**, *278*, 46046−46051.

(11) Van Der Spoel, D.; Lindahl, E.; Hess, B.; Groenhof, G.; Mark, A. E.; Berendsen, H. J. GROMACS: Fast, Flexible, and Free. *J. Comput. Chem.* **2005**, *26*, 1701−1718.

(12) Lindorff-Larsen, K.; Piana, S.; Palmo, K.; Maragakis, P.; Klepeis, J. L.; Dror, R. O.; Shaw, D. E. Improved Side-Chain Torsion Potentials for the Amber ff99sb Protein Force Field. *Proteins* **2010**, *78*, 1950−1958.

(13) Padmanabhan, S.; Baldwin, R. L. Helix-Stabilizing Interaction Between Tyrosine and Leucine or Valine when the Spacing Is i, i+ 4. *J. Mol. Biol.* **1994**, *241*, 706−713.

(14) Mcgregor, M. J.; Islam, S. A.; Sternberg, M. J. Analysis of the Relationship between Side-Chain Conformation and Secondary Structure in Globular Proteins. *J. Mol. Biol.* **1987**, *198*, 295−310.

(15) Luzar, A.; Chandler, D. Hydrogen-Bond Kinetics in Liquid Water. *Nature* **1996**, *379*, 55−57.

(16) Reidhaar-Olson, J. F.; Sauer, R. T. Combinatorial Cassette Mutagenesis As a Probe of the Informational Content o9f Protein Sequences. *Science* **1988**, *241*, 53−57.

(17) Barbas, C. F., III; Burton, D. R.; Scott, J. K.; Silverman, G. J. *Phage Display: A Laboratory Manual*; Cold Spring Harbor Laboratory Press: Cold Spring Harbor, New York, 2001.

(18) *Molecular Operating Environment*, 2013.08; Chemical Computing Group Inc.: Montreal, QC, Canada, 2013.

(19) Hess, B.; Kutzner, C.; Van Der Spoel, D.; Lindahl, E. GROMACS 4: Algorithms for Highly Efficient, Load-Balanced, and Scalable Molecular Simulation. *J. Chem. Theory Comput.* **2008**, *4*, 435−447.

(20) Essmann, U.; Perera, L.; Berkowitz, M. L.; Darden, T.; Lee, H.; Pedersen, L. G. A Smooth Particle Mesh Ewald Method. *J. Chem. Phys.* **1995**, *103*, 8577−8593.

(21) Hess, B.; Bekker, H.; Berendsen, H. J. C.; Fraaije, J. G. E. M. LINCS: A Linear Constraint Solver for Molecular Simulations. *J. Comput. Chem.* **1997**, *18*, 1463−1472.

(22) Hoover, W. G. Canonical Dynamics: Equilibrium Phase-Space Distributions. *Phys. Rev. A* **1985**, *31*, 1695−1697.

(23) Nose, S. A Unified Formulation Of The Constant Temperature Molecular-Dynamics Methods. *J. Chem. Phys.* **1984**, *81*, 511−519.

(24) Parrinello, M.; Rahman, A. A Molecular-Dynamics Study of Crystal-Structure Transformations. *Bull. Am. Phys. Soc.* **1981**, *26*, 380−380.

(25) Michaud-Agrawal, N.; Denning, E. J.; Woolf, T. B.; Beckstein, O. Software News and Updates MDanalysis: A Toolkit for the Analysis of Molecular Dynamics Simulations. *J. Comput. Chem.* **2011**, *32*, 2319−2327.

(26) Bussi, G.; Zykova-Timan, T.; Parrinello, M. Isothermal-Isobaric Molecular Dynamics Using Stochastic Velocity Rescaling. *J. Chem. Phys.* **2009**, *130*, 074101.

(27) Berendsen, H. J. C.; Postma, J. P. M.; Vangunsteren, W. F.; Dinola, A.; Haak, J. R. Molecular-Dynamics With Coupling to an External Bath. *J. Chem. Phys.* **1984**, *81*, 3684−3690.